Table III. Response Time in Function of the Hardware for an Alphanumeric Retrieval over 250 References

unit	processor	response time
two disk drives	8088 (4.7 MHz)	3 min
two disk drives	80286 (10 MHz)	1.5 min
one hard disk	80286 (10 MHz)	10 s
one virtual disk	80286 (10 MHz)	4 s

possible for this type of personalized system to acquire more diffusion among users because it solves the ordinary problems generated with the handling of increasing numbers of references.

On one side, ARIUSA can take advantage of molecular structures with a known stereochemistry; on the other side, it can take advantage of the graph theory where the stereochemistry is not considered at all but where it is possible to retrieve some new useful information. These enhancements make of ARIUSA a different personal system of chemical information, useful for a wide range of users.

ACKNOWLEDGMENT

We thank IBM of Santiago de Chile for the loan of a PC-AT microcomputer for the development of part of this work. Also, we thank DICYT of the University of Santiago de Chile and FONDECYT for financial support.

REFERENCES AND NOTES

(1) Ash, J. E.; Chubb, P. A.; Ward, S. E.; Welford, S. M.; Willet, P. *Communication, Storage and Retrieval of Chemical Information*; Ellis Horwood: Chichester, England, 1985.
(2) Smith, S. F.; Jorgensen, W. L.; Fuchs, P. L. "PULSAR: A Personalized Microcomputer-Based System for Keyword Search and Retrieval of Literature Information". *J. Chem. Inf. Comput. Sci.* **1981**, *21*, 209-213.
(3) Bonchev, D. *Information Theoretic Indices for Characterization of Chemical Structures*; Research Studies: New York, 1983.
(4) Contreras, M. L.; Deliz, M.; Galaz, A.; Rozas, R.; Sepulveda, N. "A Microcomputer-Based System for Chemical Information and Molecular Structure Search". *J. Chem. Inf. Comput. Sci.* **1986**, *26*, 105-108.
(5) Wiener, H. "Structural Determination of Paraffin Boiling Points". *J. Am. Chem. Soc.* **1947**, *69*, 17-20.
(6) Randic, M. "On Characterization of Molecular Branching". *J. Am. Chem. Soc.* **1975**, *97*, 6609-6615.
(7) Balaban, A. T.; Motoc, I. "Chemical Graphs. XXXVI. Correlations between Octane Number and Topological Indices of Alkanes". *MATCH* **1979**, *5*, 197-218.
(8) Rouvray, D. H. "Predicting Chemistry from Topology". *Sci. Am.* **1986**, *255*(3), 36-43.
(9) Platt, J. R. "Prediction of Isomeric Differences in Paraffin Properties". *J. Phys. Chem.* **1952**, *56*, 328-336.
(10) Rouvray, D. H. "The Values of Topological Indices in Chemistry". *MATCH* **1975**, *1*, 125-134.
(11) Rouvray, D. H.; Crawford, B. C. "The Dependence of Physicochemical Properties on Topological Factors". *S. Afr. J. Sci.* **1976**, *72*, 47-61.

Computer Simulation of Deuterium NMR Line Shapes

SALEM JAGANNATHAN,† FRANK D. BLUM,*,‡ and CARL F. POLNASZEK§

Applied Research Corporation, Landover, Maryland 20785, Department of Chemistry, University of Missouri—Rolla, Rolla, Missouri 65401, and Technical Computing, FMC Corporation, Minneapolis, Minnesota 55421

Received September 30, 1986

The results of a computer program written to study rotational dynamics by following the reorientation of a carbon-deuterium (C-D) bond vector in a deuteriated molecule are described. Three-dimensional plots are constructed to show how deuterium nuclear magnetic resonance splittings vary as a function of two rotational parameters. It is suggested that these diagrams provide insight into the rotational motions of the molecule.

INTRODUCTION

One of our principal research objectives is to investigate polymer dynamics by using, among other techniques, deuterium nuclear magnetic resonance (DNMR) as a probe. In contrast to the proton, deuterium has a nonzero quadrupole moment (2.73×10^{-3} barns), low abundance (0.015%), and a small magnetogyric ratio (15.3% of the proton value). Consequently, DNMR spectra are remarkably simple compared to conventional proton NMR spectra. The rationale for this is as follows: The nonzero quadrupole moment means that experimental results (relaxation times and line shapes) for deuterium can be directly related to the reorientation of C-D or O-D bond vectors. This is an intra- and not an intermolecular effect. Since C-D bonds often have axially symmetric electric field gradients, the interpretation of line shapes and relaxation times are simplified. The low abundance allows specific labeling with deuterium in any position, and it assures that the resulting DNMR spectrum only contains a contribution from deuterium in that position. The background signal from unlabeled positions is relatively negligible. This is an important advantage in concentrated solutions and bulk polymers, for example, where conventional proton NMR and ^{13}C NMR resonances may strongly overlap. Also, if only one position is labeled per monomer unit, the label does not significantly perturb the translational and rotational motion of the molecule. Finally, the relatively small magnetogyric ratio of the deuterium results in a comparatively small dipolar coupling effect. As a result of this the complicated spin-diffusion effects often seen in protonated polymers are not active in deuterium NMR.

There are many examples in the literature of how DNMR spectra are used to elucidate motions in small molecules and polymers. Jelinski et al.[1-3] have probed the anisotropic reorientation of water in an epoxy system as well as studied ring flips in collagen. Jelinski et al.[4] have also used DNMR to test the validity of "three-bond" motions in polymers. Opella et al.[5,6] have investigated ring flips and other motions in phenylalanine. Blum et al.[7] have shown how DNMR relaxation times can probe molecular motion in very concentrated polymer solutions and gels. They have also used DNMR to correlate polymer backbone dynamics with translational motion of the solvent.[8] Spiess[9,10] has described the versatility of DNMR for studying a wide variety of problems over a very wide time scale and DNMR of liquid-crystalline polymers has also been reviewed.[11]

Thus far it has proved impossible to determine molecular dynamics of systems from first principles and a combination of NMR line shapes and relaxation times. Consequently,

† Applied Research Corporation.
‡ University of Missouri.
§ FMC Corp.

0095-2338/87/1627-0167$01.50/0

mechanistic models for molecular reorientation are proposed and their results compared with experimental values. For example, the experimental spectra of absorption intensity, I, versus frequency, ω, could be compared with the theoretically simulated spectra. This approach has been used for simulation of DNMR spectra of molecules in model membrane systems.[12] In this work, we present the results of simulations based on the theory of Freed, Bruno, and Polnaszek.[13-16] In Freed et al.'s theory, the quadrupolar splitting, Δ, for a C–D bond undergoing reorientation is chiefly determined by two rotational rates, two Euler angles, and an ordering potential. The two rotational rates define the rotational diffusion of an ellipsoid with R_z (sometimes symbolized by $R_\parallel$), which could represent internal rotation of the C–D bond or a group containing the C–D bond in a molecule, and $R_x = R_y$ ($=R_\perp$), which could represent a relatively slower overall tumbling rotation of the molecule. The Euler angles α and β define the tilt of the principal axis of diffusion of the C–D bond with respect to the principal axes of the electric field gradient tensor. An ordering parameter, λ, may also be used for liquids in which molecules have a preferred axis of orientation. According to the Freed theory, Δ is a complicated function of R_z, R_x, α, β, and λ. As far as we know there exists no analytic expression for Δ as a function of the above parameters, although in certain limits, such as that of fast continuous diffusion, Δ is known. Two problems presented by Freed's theory are (a) the spectra of I versus ω for a given R_z, R_x, α, β, and λ does not reveal at a glance how Δ is affected by the latter quantities and (b) the Freed theory also does not lend itself to a rapid and simple interpretation of molecular dynamics.

It is the purpose of this paper to elucidate the first, and more modest, of the above two problems. The answer to the second, and more ambitious, problem must be postponed to a future work. In the course of our studies we have found that some insight into the effect of rotational motions of a deuteriated molecule on DNMR splitting, Δ, can be obtained by constructing three-dimensional plots, where Δ is plotted as a function of the two rotational parameters R_z and R_x ($=R_y$). The resulting figures show that Δ is a fairly sensitive function of R_z and R_x in certain regions of the three-space (Δ, R_z, R_x). Since Δ is directly influenced by molecular motion, we can also infer something about the nature of that motion from the plots. Although we have applied our idea to only a test case in this paper, the technique is nevertheless quite generally applicable under conditions different from the one chosen by us.

MODELING AND THEORY

A model of the C–D is shown schematically in Figure 1. The principal axes of the electric field gradient tensor, V, of the deuterium are denoted by x, y, and z. Two of the three Euler angles, α and β, define the tilt of the principal diffusion axis R_z (the third Euler angle, γ, is zero for axially symmetric rotational diffusion) with R_x and R_y being perpendicular to R_z. For the present case, we have chosen a C–D bond with zero asymmetry parameter, $\eta = 0$ [$\eta = (V_{xx} - V_{yy})/V_{zz}$ by definition], but the theory is general and applicable to any X–D bond vector.

The effect of rotational motions of a C–D bond, in a molecule undergoing reorientation, upon its absorption spectrum is theoretically investigated here by employing the stochastic Liouville method of Freed et al.[13-16] While other theories also exist in the literature, such as those of Alexander et al.,[17] Spiess,[18] and Kothe et al.,[11] we have chosen the Freed theory as most appropriate to the task at hand. A complete comparison of the different theories remains to be carried out.[19] The Freed theory is lengthy and complicated. Rather than describe it thoroughly we will simply summarize the salient

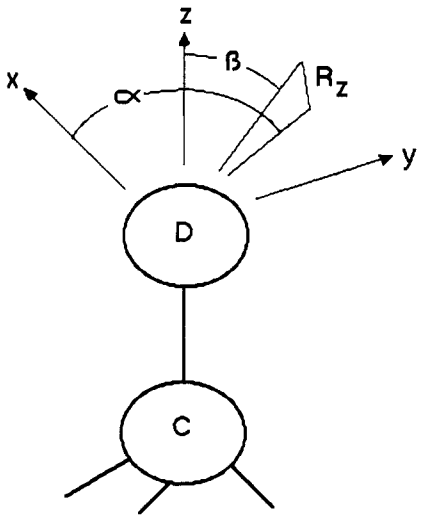

Figure 1. Schematic representation of a C–D bond group (based on a similar diagram in ref 11). x, y, and z represent the principal axes of the electric field gradient tensor of deuterium. R_z is the principal axis of diffusion (for clarity the R_x and R_y axes, which are perpendicular to the R_z axis, are omitted from the figure). α and β are Euler angles denoting tilt of R_z.

features here. A detailed review of the theory[13] has appeared, and it may be consulted for further information. The starting point is the stochastic Liouville equation for the density matrix $\rho(t)$

$$\partial \rho(\Omega,t)/\partial t = i[\mathcal{H}(\Omega),\rho(\Omega,t)] - \Gamma_\Omega \rho(\Omega,t) \qquad (1)$$

where $\Omega = \alpha, \beta, \gamma$ represents the Euler angles specifying orientation of spins, Γ_Ω is a Markovian rotational diffusion operator, and $\mathcal{H}(\Omega)$ is the spin Hamiltonian. The steady-state spectrum is obtained by Fourier analyzing the above equation, i.e., by letting $(\rho - \rho_0)_\lambda = \sum_{n=-\infty}^{\infty} e^{in\omega t} Z_\lambda^{(n)}(\Omega)$, where ρ_0 is the equilibrium density matrix and λ is a label for transition. This leads to an algebraic equation for $Z_\lambda^{(n)}(\Omega)$, where $Z_\lambda^{(n)}$ is the nth harmonic complex Fourier coefficient. The equilibrium average, $\langle\ \rangle_{eq}$, of the imaginary part of the $n = 1$ harmonic $\langle \mathrm{Im}\ Z_\lambda^{(1)} \rangle_{eq}$ is directly proportional to the power absorbed in the λth transition, P_λ:

$$P_\lambda \propto h\omega\ \langle \mathrm{Im}\ Z_\lambda^{(1)}(\Omega) \rangle_{eq} \qquad (2)$$

For mathematical convenience $Z_\lambda^{(n)}$ is "symmetrized" to $Z_\lambda^{(n)*}(\Omega)$, and this quantity is further expanded in a basis set of complete orthonormal functions $G_m(\Omega)$

$$Z_\lambda^{(n)*}(\Omega) = \sum_m [C_m^{(n)}(\omega)]_\lambda G_m(\Omega) \qquad (3)$$

where ω is the angular frequency. Substituting the above truncated expansion into the algebraic equations for $Z_\lambda^{(n)*}$ gives a set of coupled algebraic equations for $[C_m^{(n)}]_\lambda$. The numerical solution of the latter equations completes the objective of Freed's theory and leads to the full absorption spectrum, $I(\omega)$. A FORTRAN computer program has been written by one of us (C.F.P.) to do just this. It is found that I is sensitively dependent on the eigenvalues of the rotation diffusion operator Γ_Ω, where for axially symmetric Brownian motion (applicable in this work)

$$\Gamma_\Omega \Phi_{KM}^L = [R_x L(L+1) + (R_z - R_x)K^2]\Phi_{KM}^L \qquad (4)$$

where R_x and R_z are the rotations described earlier and Φ_{KM}^L are the normalized Wigner rotation matrices.[20] I also depends upon $\Omega = \alpha, \beta$, and γ, the Euler angles. Finally, Freed's theory is capable of dealing with a liquid that has a preferred axis of orientation by introducing an ordering potential $V(\alpha,\beta)$, where

$$-V(\alpha,\beta)/kT = \lambda \cos^2\beta + \sigma \sin^2\beta \cos 2\alpha \qquad (5)$$

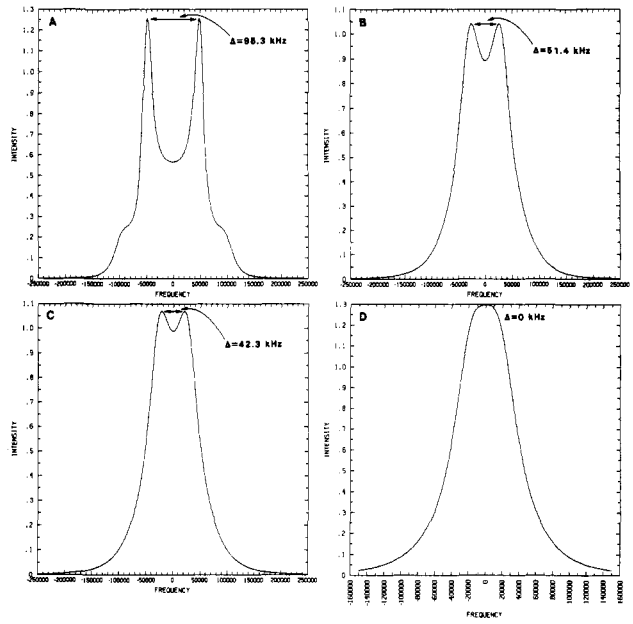

Figure 2. Theoretically simulated DNMR absorption spectra, where I is the absorption intensity and ω is the angular frequency in hertz (Hz). The parameters α, β (tilt angles), γ (ordering parameter), e^2qQ/h (static quadrupole coupling constant) and L,K (truncation parameters, cf. eq 4 in text) used in the simulations have the values 0°, 20°, 0, 168 kHz, and 24, 14, respectively. An intrinsic (or residual) line width of 20 Hz was used in the simulations. Panels A–D illustrate a sequence of spectra for the same molecule with a fixed value of $R_z = 10^5$ s^{-1} and the following increasing values of R_x: (A) 6×10^3 s^{-1}; (B) 6×10^4 s^{-1}; (C) 7×10^4 s^{-1}; (D) 10^5 s^{-1}. Note that while the frequency scan range for (A)–(C) is 500 kHz, it is 320 kHz for (D).

with λ and σ being certain ordering parameters. In this case $I(\omega)$ is also sensitive to the ordering parameters.

The theory described above was originally applied to the simulation of electron spin resonance (ESR) spectra of free radicals. However, by invoking the formal equivalence[21] between ESR spin = 1 zero field splitting and the quadrupole interaction in NMR for spin = 1 nuclei, one can extend the theory to DNMR spectra as well. A crucial assumption of the Freed theory that results in enormous simplification in computing $I(\omega)$ is this: while in general $I(\omega)$ would be affected by fluctuations in the Euler angles Ω due to overall reorientational motion as well as the internal rotation of the C–D bond vector, Freed has shown[22] that one can naively assume that all rotational motions are decomposable in terms of only *two* types of rotations, R_z, representing the *net* effect of relatively rapid internal rotations, and R_x and R_y, representing the *net* effect of slow overall motion. Of course there must be cases where such a simplified model will fail. Thus, we have not always been able to simulate experimental spectra. Kothe et al.,[11] for example, have included trans-gauche chain isomerizations in their model. In principle, it is possible to simulate almost any type of motion.

SIMULATIONS

By applying Freed's theory to a C–D bond vector undergoing reorientation, we have simulated DNMR absorption spectra, giving Δ, splitting in kilohertz (kHz), as a function of R_z and R_x, mutually perpendicular rotational rates in reciprocal seconds. In order to illustrate the quality of our simulations we refer to Figure 2. Panels A–D are simulated DNMR spectra for a sequence of R_xs with a fixed R_z (the values of these and the other parameters used in the simulation are stated in the caption to Figure 2). It is seen that the splitting Δ falls from a nonzero value of 96.3 kHz at $R_x = 6 \times 10^3$ s^{-1} to zero at a faster tumbling rate of $R_x = 10^5$ s^{-1}, as is quite reasonable. The shapes of the spectra are also realistic.

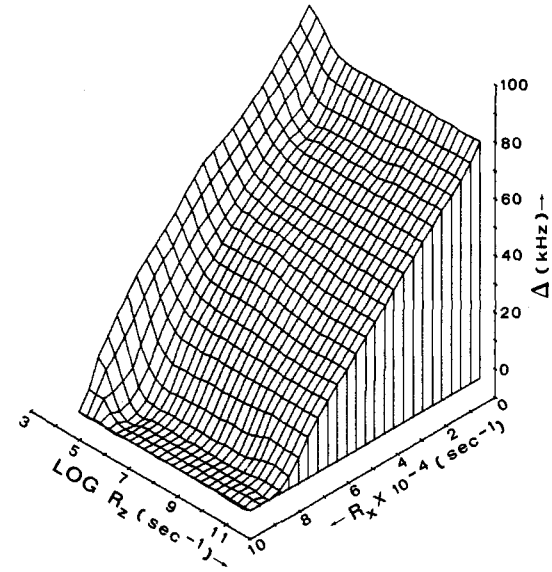

Figure 3. Three-dimensional plot of Δ, the DNMR splitting, versus R_z and R_x representing the principal axes of diffusion with R_z perpendicular to R_x. The parameters α, β (tilt angles), γ (ordering parameter), and e^2qQ/h (static quadrupole coupling constant) have the same values as stated in the caption for Figure 2.

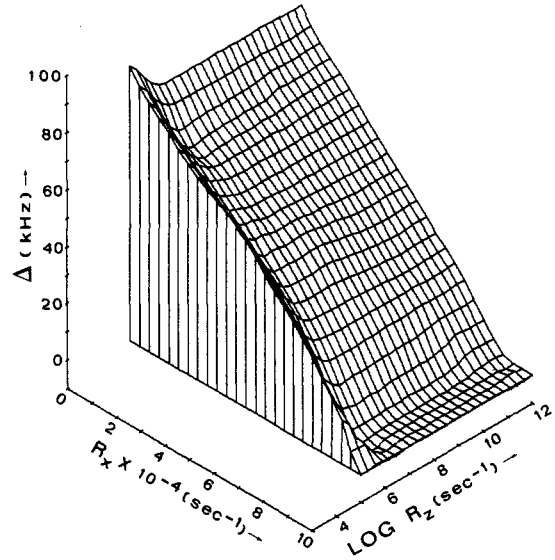

Figure 4. Different view of the plot in Figure 3 looking at it from the direction of the "negative" R_z axis.

In the preceding simulations the tilt angle β was arbitrarily chosen to be 20°. In general the splitting is maximum for $\beta = 0°$ and vanishes at the "magic angle" value of $\beta = 54.74°$ (we have set $\alpha = 0°$ in these and following calculations).

These and the other data are displayed, with the help of TEMPLATE Graphics routines,[23] in the form of surface plots in the three-space (Δ, R_z, R_x), as shown in Figures 3 and 4 for two different viewpoints. What is immediately apparent from, say, Figure 3, is that Δ is a reasonably smooth function of R_z and R_x. It is also clear that Δ is much more sensitive to small changes in R_x, denoting overall rotation of the molecule, than it is to R_z, denoting relatively rapid ($R_z \geq R_x$) motion of the C–D bond. In the example chosen by us the smallest value of R_x is equal to 6×10^3 s^{-1}, sufficient for the task at hand. We could have displayed Δ for smaller values of R_x except that for smaller R_x values more CPU time is required to calculate a corresponding Δ. The generation of each data point or a Δ for a given pair (R_z, R_x) required about 30 min of CPU time per point on a PRIME 550-II computer using a FORTRAN program written by one of us (C.F.P.). Then these

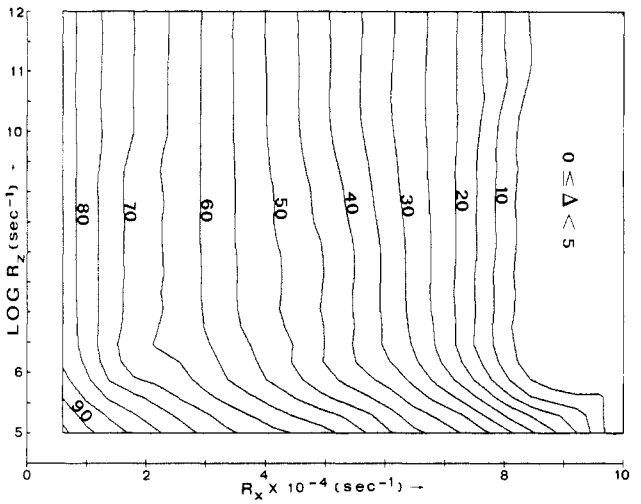

Figure 5. Contour diagram for the plot in Figure 3. Δ value in kilohertz is indicated on each of the equally spaced contour lines.

data points were interpolated by using a bivariate interpolation scheme, which is available as a TEMPLATE packaged program, so as to obtain a reasonable number of points (Δ, R_z, R_x) to be plotted by a TEMPLATE surface plot generator. Since the latter also has the capacity to rotate an object under view, we have shown, in Figure 4, another view of the same plot as in Figure 3. In order to read off values of Δ corresponding to any (R_z, R_x), it is convenient to have a contour plot. This we have generated, as shown in Figure 5, also with the help of yet another TEMPLATE routine.

What can be deduced about the nature of molecular motion from these figures? Depending on where one is on the (Δ, R_z, R_x) surface, it is possible to say how rapidly the molecule is tumbling; if the tumbling rate, R_x, is quite fast, 10^5 s^{-1} or greater, in this instance, then the effect of rapid internal rotations, denoted by R_z, has no discernable effect on the quadrupolar splitting. On the other hand, at tumbling rates smaller than 10^5 s^{-1}, internal rotations begin to affect quadrupolar splitting patterns. Thus, we see from the contour plot (Figure 5) that for $R_z > 10^6$ s^{-1} there is a 5 kHz stepwise increase in the splitting, Δ, for every stepwise decrease in the R_x rate of 3000–5000 s^{-1}. While the precise prediction of rotational motions must vary depending on what parameters one has chosen for the theoretical simulation, it is clear that these three-dimensional plots offer a visual insight into the broad effects involved and to the extent that we have demonstrated that our aim is fulfilled.

CONCLUSIONS

We have suggested a technique for obtaining insight into molecular rotational motions by using three-dimensional plots of quadrupolar splitting, Δ, versus two rotational parameters, R_z and R_x, described in the text. Although the data required to construct these diagrams require, at present, more than a modest amount of CPU time, the technique has, nevertheless, very useful consequences for polymer dynamics research. Recently, Freed et al.[24] have suggested ways to speed up the most time-consuming step, which is the generation of Δ for a given pair (R_z, R_x), by using the Lanczos algorithm (already implemented by Kothe et al.[11]). This should make our technique even more attractive.

ACKNOWLEDGMENT

We thank the donors of the Petroleum Research Fund, administered by the American Chemical Society, for their financial support. We also thank Mark Cain for help with the computation and the Drexel University Center for Scientific Computation for providing computer time.

REFERENCES AND NOTES

(1) Jelinski, L. W.; Dumais, J. J.; Stark, R. E.; Ellis, T. S.; Karasz, F. E. *Macromolecules* **1983**, *16*, 1021.
(2) Jelinski, L. W.; Sullivan, C. E.; Torchia, D. A. *Nature (London)* **1980**, *284*, 531.
(3) Jelinski, L. W.; Sullivan, C. E.; Batchelder, L. S.; Torchia, D. A. *Biophys. J.* **1980**, *32*, 515.
(4) Jelinski, L. W.; Dumais, J. J.; Engel, A. K. *Macromolecules* **1983**, *16*, 1492.
(5) Gall, C. M.; DiVerdi, J. A.; Opella, S. J. *J. Am. Chem. Soc.* **1981**, *103*, 5039.
(6) Frey, M. H.; DiVerdi, J. A.; Opella, S. J. *J. Am. Chem. Soc.* **1985**, *107*, 7311.
(7) Blum, F. D.; Durairaj, B.; Padmanabhan, A. S. *Macromolecules* **1984**, *17*, 2837.
(8) Blum, F. D.; Padmanabhan, A. S.; Durairaj, B. *J. Polym. Sci., Polym. Phys. Ed.* **1986**, *24*, 493.
(9) Spiess, H. W. *Colloid Polym. Sci.* **1983**, *261*, 193.
(10) Spiess, H. W. *Pure Appl. Chem.* **1982**, *57*, 1617.
(11) Muller, K.; Meier, P.; Kothe, G. *Prog. Nucl. Magn. Reson. Spectrosc.* **1985**, *17*, 211.
(12) Stockton, G. W.; Polnaszek, C. F.; Tulloch, A. P.; Hasan, F.; Smith, I. C. P. *Biochemistry* **1976**, *15*, 954.
(13) Freed, J. H. In *Spin Labeling: Theory And Applications*; Berliner, L., Ed.; Academic: New York, 1976; Chapter 3 and references therein. This is a review paper covering the applications of the Freed et al. theory up to 1975. Also included is a program to compute electron spin resonance line shapes.
(14) Campbell, R. F.; Meirovitch, E.; Freed, J. H. *J. Phys. Chem.* **1979**, *83*, 525.
(15) Meirovitch, E.; Freed, J. H. *Chem. Phys. Lett.* **1979**, *64*, 311.
(16) Schwartz, L. J.; Meirovitch, E.; Ripmeester, J. A.; Freed, J. H. *J. Phys. Chem.* **1983**, *87*, 4453.
(17) Alexander, S.; Baram, A.; Luz, Z. *Mol. Phys.* **1974**, *27*, 441.
(18) Spiess, H. W. *J. Chem. Phys.* **1986**, *84*, 4579. See, especially, the Appendix.
(19) For a comparison of older theories the following two monographs may be consulted: Abragam, A. *The Principles of Nuclear Magnetism*; Oxford University: Oxford, U.K., 1985. Mehring, M. *High Resolution NMR Spectroscopy in Solids*; Springer: Berlin, 1976.
(20) Rose, M. E. *Elementary Theory of Angular Momentum*; Wiley: New York, 1957.
(21) Freed, J. H.; Bruno, G. V.; Polnaszek, C. F. *J. Chem. Phys.* **1971**, *55*, 5270.
(22) Mason, R. P.; Polnaszek, C. F.; Freed, J. H. *J. Phys. Chem.* **1974**, *78*, 1324.
(23) TEMPLATE Graphics Package, Megatek Corp., San Diego, CA.
(24) Moro, G.; Freed, J. H. *J. Chem. Phys.* **1981**, *74*, 3757.